Available online at www.sciencedirect.com
ScienceDirect
Journal of Power Sources 162 (2006) 198–206
JOURNAL OF POWER SOURCES
www.elsevier.com/locate/jpowsour

High performance direct ammonia solid oxide fuel cell

G.G.M. Fournier [a,*], I.W. Cumming [a], K. Hellgardt [b]

[a] *Chemical Engineering Department, Loughborough University, Loughborough, Leicestershire LE11 5BG, United Kingdom*
[b] *Department of Chemical Engineering and Chemical Technology, Imperial College of Science, Technology and Medicine, London SW7 2AZ, United Kingdom*

Received 28 February 2006; received in revised form 15 May 2006; accepted 9 June 2006
Available online 26 July 2006

Abstract

Yttria stabilized zirconia (YSZ) and calcia stabilized zirconia (CaSZ) electrolyte materials were tested in an intermediate temperature fuel cell using ammonia as a fuel. Silver, platinum and a nickel cermet were used as anode materials in an annular and a pellet design. At 800 °C, the nickel cermet achieved ammonia conversions of more than 90%, significantly higher than those obtained with silver and platinum. Direct conversion of ammonia at 800 °C, resulted in a power density of 60 mW cm^{-2} at a current density of 200 mA cm^{-2}, for a pellet system with a nickel cermet anode, and a silver cathode and employing an 8 mol% YSZ electrolyte (thickness of 400 μm).

A direct comparison of the performance of a cell running on either hydrogen or ammonia showed that with ammonia the cell generates slightly higher power densities when using a nickel cermet anode. This phenomenon is explained using the Nernst equation, involving the relevant activities at the electrode surface.

A comparison of the different oxide ion conducting systems studied under direct ammonia fuel operation shows the high potential of ammonia.

Keywords: Ammonia; High performance; Solid oxide fuel cell; Nickel cermet; Yttria stabilized zirconia

1. Introduction

New requirements for low emissions and the pressing need to be less dependent on foreign oil have favoured the search for alternative technologies and alternative fuels such as biodiesel. Solutions must offer a sustainable development, high-energy efficiency, an easy management (start up and shut down) and low emissions. Fuel cells are a radically new and fundamentally different way of making electrical power from a variety of fuels.

A lot of attention is being given to high temperature fuel cells and more precisely solid oxide fuel cells (SOFC) as they have the highest potential for development. They exhibit high efficiencies and fuel flexibility [1]. For many years, people thought that the best application for solid oxide fuel cells was large-scale (power plants of 100 kW and over). Recent developments have shown that the technology can be applied to small-scale units and portable applications [2]. Several designs have been developed for SOFCs, tubular and planar being the most studied and furthest advanced [1,3], both of them showing very promising performance.

However SOFCs, as well as having high efficiencies, have a higher operating temperature that allow the use of fuels that are alternative sources of hydrogen [4]. Hydrogen is a common choice of fuel but it presents several problems, its safe handling being one of the most important. Another problem associated with the use of hydrogen is the development of a worldwide distribution network needing considerable investment. Numerous fuels have been used as substitutes for hydrogen, the main ones being methanol, methane and solid biomass. Natural gas has also been considered but there is a problem of catalyst poisoning with the production of CO and the storage of natural gas for mobile and small-scale power units is only possible as LPG. In this study, we have considered the alternative of ammonia which is becoming of increasing interest to fuel cell researchers.

Ammonia is produced via the well-known Haber–Bosch process. It is distributed worldwide as it is used in many applications such as fertilizer manufacture. Ammonia is after sulphuric acid the most produced commodity chemical. The technology is

* Corresponding author. Tel.: +44 7789 731 493; fax: +44 1509 223 923.
E-mail addresses: g.g.m.fournier@lboro.ac.uk (G.G.M. Fournier), i.w.cumming@lboro.ac.uk (I.W. Cumming), k.hellgardt@imperial.ac.uk (K. Hellgardt).

0378-7753/$ – see front matter © 2006 Elsevier B.V. All rights reserved.
doi:10.1016/j.jpowsour.2006.06.047

Nomenclature

f_i	fugacity coefficient
P	pressure in the system (Pa)
P_c	critical pressure
R	gas constant (8.314411 J mol^{-1} K^{-1})
T	temperature in the system (K)
T_c	critical temperature
V_i	volume (m^3)
ϕ_i	fugacity

mature and the scale up is relatively easy. The global production capacity approximated 170.8 million tonnes in 2004–2005 [5]. Ammonia production prices have fluctuated over the past several years. In 2002, ammonia prices were around US$ 250 per tonne while current prices are approximately US$ 350–375 per tonne [6], while the current prices for hydrogen range from US$ 800–3400 per tonne [7]. The production price of ammonia equates to roughly US$ 1.2 kWh^{-1}, for comparison methanol costs US$ 3.8 kWh^{-1} and hydrogen US$ 25.4 kWh^{-1} [8].

In terms of safety, ammonia poses a low risk of ignition in the presence of sparks or open flames. A flammability limit is given for ammonia but generally it is considered to be a non-flammable gas [9]. The main concern associated with ammonia is a health issue as ammonia is harmful, but its specific smell makes it very easy to detect in cases of leaks so preventative measures can be taken. Furthermore, any releases of ammonia would be immediately dispersed. Ammonia injection is being used by the power industry to mediate NO_x emissions. Beyond the safety issue, ammonia's good thermodynamic properties and low production costs make it a very attractive fuel for fuel cell applications. A direct comparison between hydrogen and ammonia properties easily demonstrates the benefits of using ammonia. Ammonia can be easily stored at room temperature when a pressure of 8.6 bars is applied; in the case of hydrogen an extremely low temperature of 20 K and high cost tanks are required to keep it in its liquid form. Ammonia is a suitable hydrogen carrier (hydrogen capacity larger than for liquid hydrogen), the usable hydrogen per kilogram of ammonia is relatively high compared to other hydrogen generation approaches. A recent study conducted by Christensen et al. [10] has demonstrated the high potential of ammonia as a source of hydrogen for fuel cells. They have developed a new technology to store ammonia using metal ammine salts. These offer a safe, reversible, high density and low cost solution to ammonia storage. The development of this new technology could provide a cheap alternative to expensive high pressure hydrogen storage tanks or low pressure ammonia tanks. Ammonia exhibits another advantage over hydrogen and fuels such as propane, methanol and solid biomass. It presents the highest power release per litre of fuel, 1.45 kWh l^{-1}. It is also important to point out that its decomposition occurs at the operating temperatures of solid oxide fuel cells (773–1273 K) according to the following equation [11]:

$$NH_3 \rightarrow \tfrac{1}{2}N_2 + \tfrac{3}{2}H_2, \quad \Delta H = 46.22\,\text{kJ mol}^{-1}$$

Ammonia cracking is an easy process while hydrocarbons or biomass require a reformer unit to convert the source fuel into hydrogen, carbon monoxide and carbon dioxide, the last two being greenhouse effect gases. In addition to this extra unit, it is essential to remove impurities present in the source fuel as they could damage the catalyst used in the fuel cell. The use of alternative fuels such as biomass and methanol by internal reforming route is currently being investigated to avoid these problems. No high cost catalysts are required to reach high conversion of ammonia. Nickel has been proven to be a very efficient catalyst, and almost complete conversion can be achieved at temperatures above 773 K [4,12]. Furthermore, there is no emission associated with the use of ammonia apart from nitrogen on the anode and water on the cathode side. This internal reforming process of ammonia has to be carefully designed depending on the geometry and stack design. Furthermore, the performance of the fuel cell will directly depend on the efficiency of the internal reforming as the amount of hydrogen produced will vary with it.

Ammonia has recently been investigated using high temperature proton conductor systems [14] as well as several oxide ion-conducting systems [13,15]. In all cases, ammonia showed high performance, very close to that of hydrogen at intermediate temperatures. However, these studies do not offer an extensive review of the possibilities of a direct ammonia fuel cell. Wojcik et al. [13] investigated the use of ammonia in annular system using silver and platinum as electrode material showing the potential of internal reforming of ammonia. Dekker et al. [15] only covered the high current density range therefore not showing the whole potential of ammonia.

In this paper, a detailed experimental investigation of the characteristics of ammonia fuel cells has been carried out to determine the optimal operating conditions and design parameters for the implementation of direct ammonia fuel cells. We investigated and compared the performance of two different designs: an annular and a planar cell. Three different electrode materials: silver, platinum and a nickel cermet were used and studied over the whole range of current densities and demonstrate that a direct ammonia fuel cell generates higher power densities than a hydrogen powered fuel cell.

2. Experimental

2.1. General set-up

The present study was conducted using ammonia as fuel and argon as carrier gas in a solid oxide fuel cell using two different electrolyte designs: a tubular structure and a simpler, planar one.

A general schematic of the complete test system is given in Fig. 1.

2.2. Tubular set-up

In the tubular set-up an electrolyte tube formed part of an annular reactor. Two types of electrolyte material were used for the preparation of the cell, the first one being 12 mol% calcia stabilized zirconia (CaSZ) and the second one 6 mol% yttria stabilized zirconia (YSZ). The tube dimensions, Table 1, were

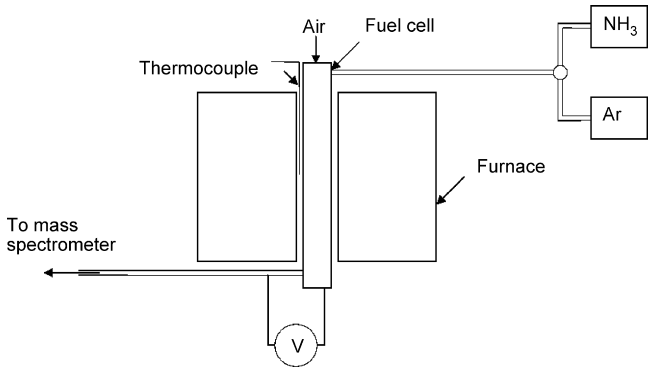

Fig. 1. Experimental set-up.

Table 1
Dimensions of the electrolyte tubes

Dimensions	12 mol% CaSZ	6 mol% YSZ
Length	28 cm	32 cm
Wall thickness	1.05 mm	1.05 mm
Diameter	6 mm	6.1 mm

similar making it possible to compare the performance of the different materials.

The YSZ tubes were supplied by Vesuvius Ltd. (US) and the calcia stabilized tubes by Reetz Materials, GmbH (Germany). The electrode materials were silver paint from Thomas Wolbring GmbH (Germany), platinum paint from Gwent Electronics (UK) and a NiO–YSZ cermet tape supplied by ESL Electro Science (UK) allowing for several electrode combinations. Silver was used as cathode material in all cases.

2.2.1. Preparation and deposition of electrodes

The deposition of the silver electrodes was done using two different methods. The cathode and the anode were deposited, respectively onto the inner and the outer surfaces of the tube. The silver was supplied as a thick paint, which was diluted using a silver paint diluent: iso butyl methyl ketone. The deposition on the inner surface of the tube was done by placing a pipette filler on top of the tube and sucking the silver solution into the tube. The paint was then left to drain. The deposition of the silver on the outer surface of the tube was performed by using an air spray gun allowing good control of the amount of paint deposited. The coating was left to dry over night and then fired at 873 K for 2 h in air.

To make a platinum anode, paint was applied using a brush. The paint was dried at 423 K for 5 min using a blow dryer and was fired at 1173 K for 2 h.

The NiO–YSZ anode tape material is cadmium and lead free tape supplied in green form. It was applied onto the tube by simply wetting the surface of the electrolyte with a solvent, dowanol and quickly placing the tape onto the tube. The system was then sintered in air at 1773 K for 6 h.

In order to make the electrical connection for the voltage measurements and to apply the load on the cell, an extra coating needed to be applied at one end of the electrolyte tube to ensure the connection with the inside of the tube as shown in Fig. 2.

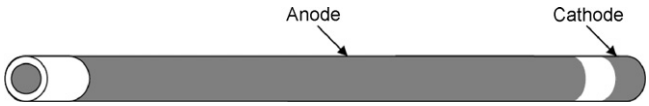

Fig. 2. Schematic of the tube with the anode and the cathode.

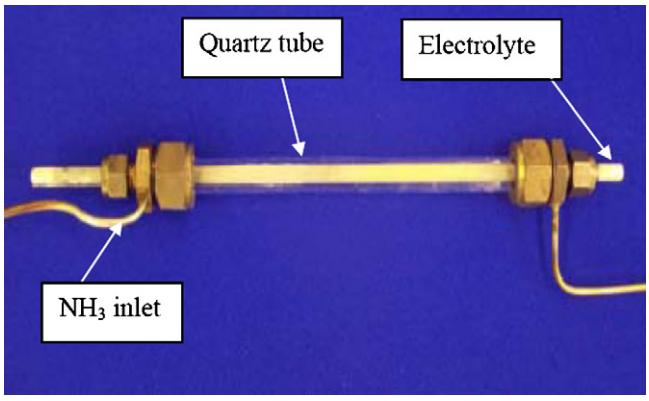

Fig. 3. Picture of the cell assembly.

In order to avoid any short-circuiting problems, it was made sure that the surface covered was not in contact with the anode as shown on the picture. The total active surface area of the electrodes was 32 cm^2.

2.2.2. Assembly of the cell

One of the most important points of the design is to ensure that there is no contact between the atmospheres of the anode and the cathode. A quartz tube was therefore used on the anode side, Fig. 3. The quartz tube and the electrolyte tube were assembled to form the main body of the cell.

The study of the fuel cell performance was carried out over a wide range of temperatures, from 773 to 1073 K, controlled by a thermocouple in contact with the cell placed inside the furnace. The cell was connected to a mass spectrometer to analyse the composition of the exit gases.

2.3. Pellet reactor

The experimental apparatus employed for the electrocatalytic measurements was a two-chamber reactor. The electrolyte pellet was prepared from an 8 mol% yttria stabilized zirconia powder supplied by Unitec Ceramics (UK). The powder was ground in a mortar with a pestle for 5 min to eliminate any agglomerates. The powder was then pressed into pellets at a pressure of 50 MPa. The resulting pellets were sintered in air at 1773 K for 6 h. They were polished using a fine diamond brush to obtain a smooth and clean surface. This also allowed the production of several thickness from 1.5 to 0.4 mm. The chosen pellet for the experiments had a thickness of 0.4 mm.

The reactor consisted of a non-porous alumina tube with an inside diameter of 16 mm, an outside diameter of 20 mm and a length of 30 cm. The tube was open at both ends, at one end two tubes were fitted, one for the ammonia feed and the other for the escape of the reaction products, N_2, water and any unreacted feed gas, Fig. 4.

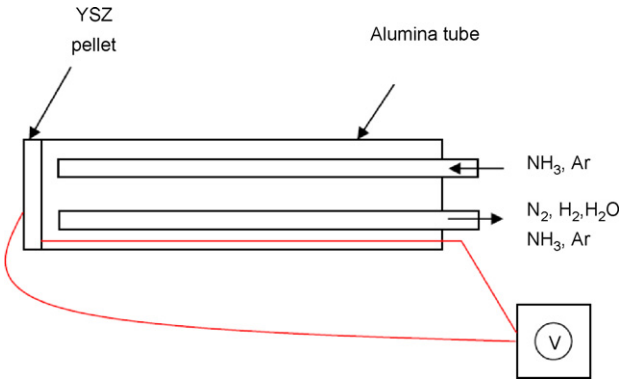

Fig. 4. Schematic of the reactor.

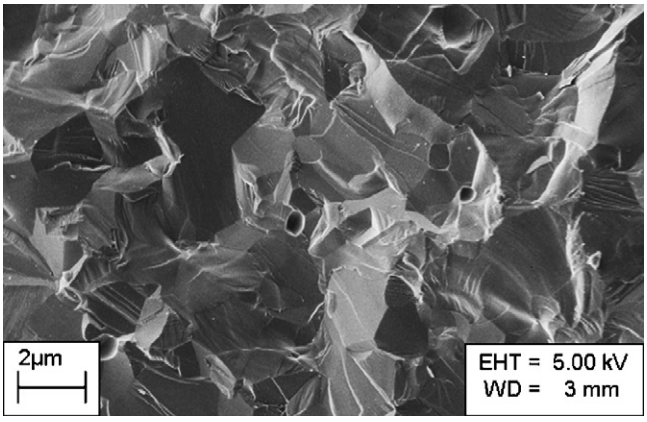

Fig. 5. SEM photograph of the cross-section of a YSZ pellet sintered at 1773 K.

At the other end of the tube a pellet of yttria stabilized zirconia was fitted. Two electrode films were deposited on either side of the disk. The electrode materials were silver on the air side and the NiO–YSZ tape on the ammonia side. The total surface area of the electrodes was 1.5 cm^2. The pellet was fixed to the end of the tube using a high temperature resisting sealant (Autostic, FC6, provided by Fortafix). The sealant was an alkali silicate glass, non-conducting paste, applied with a brush. Once the cement was dry, the reactor was fired at 873 K for 2 h. It was then tested for leaks. The current collector for the anode was painted on the inside of the support tube. For the cathode, the current collector was a silver wire connected to the cathode using silver paint. A schematic of the reactor is given in Fig. 4.

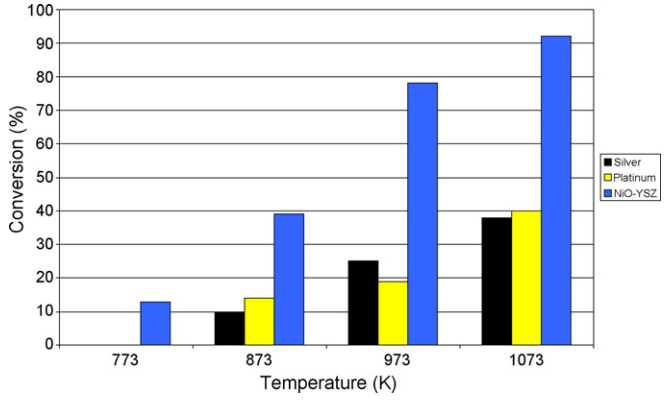

Fig. 6. Ammonia conversion for different anode materials.

Before the pellets were tested at operating conditions, they were examined using scanning electron microscopy (SEM) for microstructure. As shown on Fig. 5, fully dense samples were produced, calculations of the relative densities confirmed these results. Relative densities of more than 93% were achieved after annealing at 1773 K for 6 h. The theoretical density was calculated to be 5.958 g cm^{-3}.

3. Results and discussion

3.1. Tubular reactor

3.1.1. Influence of the anode material on the ammonia conversion

Conversions for the three different anode materials were determined at open circuit conditions once steady state had been reached. Both ammonia and argon flow rates were kept constant at 24 ml min^{-1}, equivalent to a concentration of ammonia of 50%, during the series of experiments. The ammonia conversion was measured using a mass spectrometer. To do this, both the ammonia content of the incoming and discharge gases were analysed.

Conversions were determined according to:

$$X_{NH_3} = \frac{N_{NH_3,in} - N_{NH_3,out}}{N_{NH_3,in}} \quad (1)$$

Fig. 6 gives a comparison of the ammonia conversions achieved over different anode materials. Platinum and silver appear to give similar conversions whereas the nickel cermet shows much higher levels of decomposition of ammonia at all temperatures. At 773 K, negligible conversion is obtained for silver and platinum, less than 1% of the ammonia that is fed to the cell is converted into hydrogen and nitrogen. The conversion increases slowly with the temperature to reach 38% at 1073 K. This agrees with the poor performance of a direct ammonia fuel cell with silver electrodes shown by Wojcik et al. [13]. In contrast, the nickel cermet, exhibits very good results especially at high temperatures. At 773 K, already 13% of the ammonia present in the feed to the cell is decomposed, and the conversion reaches 92% at 1073 K. The data collected confirm the results previously obtained during studies of ammonia decomposition, demonstrating the catalytic activity of nickel for ammonia decomposition [12]. This suggests that nickel cermet as anode material is one the most suitable candidates for use in direct ammonia fuel cells. Other good candidates are ruthenium and iridium; Choudhary and Goodman [16] have demonstrated that 99% conversion can be achieved at 923 K using a 10% Ru/SiO_2 catalyst and 98% conversion is reached at 973 K with a 10% Ir/SiO_2.

At operating conditions of 1073 K and when a load was applied to the cell, the cell delivered an EMF of 0.5 V with a current density of 18 mA cm^{-2}, 20% of the hydrogen produced was used to generate the current and produce water, and the rest was in the exit gas.

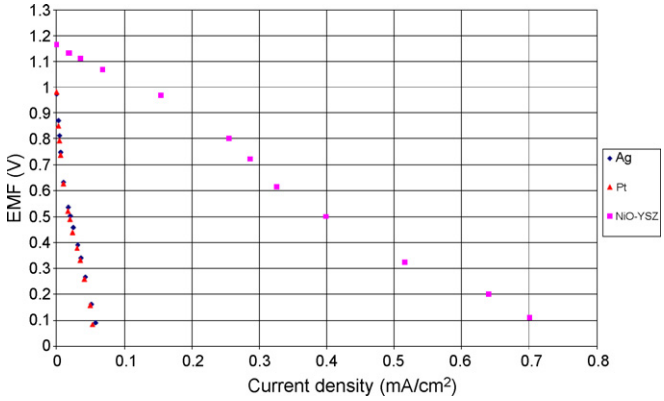

Fig. 7. *I–V* curves of NiO–YSZ/YSZ/Ag, Pt/YSZ/Ag and Ag/YSZ/Ag with ammonia as source fuel at 773 K.

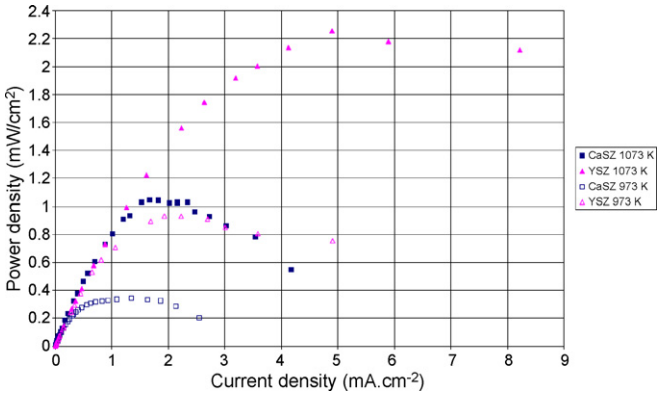

Fig. 9. Power density curves comparison between YSZ and CaSZ using silver electrodes.

3.1.2. *Influence of the anode material on the performance of the cell*

From the results obtained for the conversion of ammonia, it is expected that the nickel will exhibit significantly higher current densities than silver and platinum at every operating temperature and the latter two materials should exhibit similar performance.

Fig. 7 illustrates that this is indeed the case at 773 K; the cell with the cermet achieves current densities almost 10 times higher than that for the other cells. At this temperature, the ammonia conversion did not even reach 1% for silver and platinum, meaning that almost no hydrogen was present in the system. This explains the very low current densities of less than 0.1 mA cm^{-2}. At 1073 K as shown in Fig. 8, the performance of the cells with platinum and silver anodes is much closer to that of the nickel anode. The increase in ammonia decomposition is responsible for this change but there is still a factor 5 between the nickel anode and the precious metals. This, therefore, suggests that nickel cermet is one the most appropriate material. Ruthenium and iridium are yet to be tested for direct ammonia fuel cells to confirm their high activity towards ammonia. Other noble metals such as silver and platinum are not best suited for ammonia decomposition and therefore fuel cell design.

3.1.3. *Comparison between calcia stabilized zirconia and yttria stabilized zirconia*

Two cells were prepared to compare the properties of the two electrolyte materials. The electrodes were identical (silver). Fig. 9 clearly shows the difference in cell performance resulting from the different properties of YSZ and CaSZ. At 800 °C, 12 mol% CaSZ and 6 mol% YSZ exhibit resistivities of 200 Ω cm and 30 Ω cm, respectively [17,18]. The reaction rate on the anode side is dependent on the rate of oxygen transferred. YSZ exhibits a much faster oxygen transport and this explains the significant difference in terms of power density between the two systems for a given flow of ammonia.

3.1.4. *Influence of the flow rate*

The flow rate of ammonia appears to have a significant impact on the behaviour of the cell when using calcia stabilized zirconia as electrolyte material. As the current density increases the potential of the cell drops much quicker for low flow rates as shown on Fig. 10. This is particularly true for a flow of 6 ml min^{-1}. This effect is probably due to the lack of hydrogen present in the system because of the low conversion obtained with silver. At a flow of 24 ml min^{-1} there is four times more hydrogen being produced in the reactor than at 6 ml min^{-1}, which explains why the voltage drop is not present anymore.

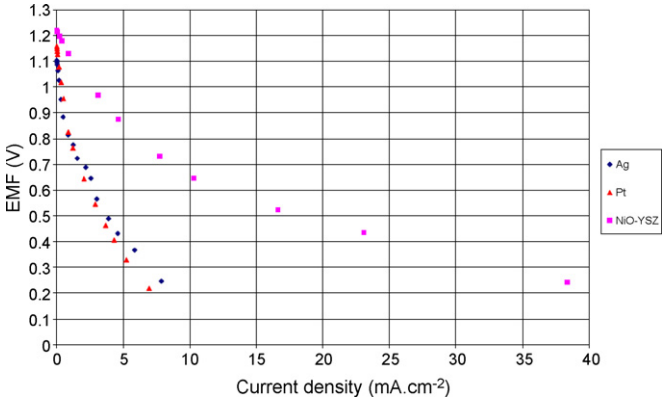

Fig. 8. *I–V* curves of NiO–YSZ/YSZ/Ag, Pt/YSZ/Ag and Ag/YSZ/Ag with ammonia as source fuel at 1073 K.

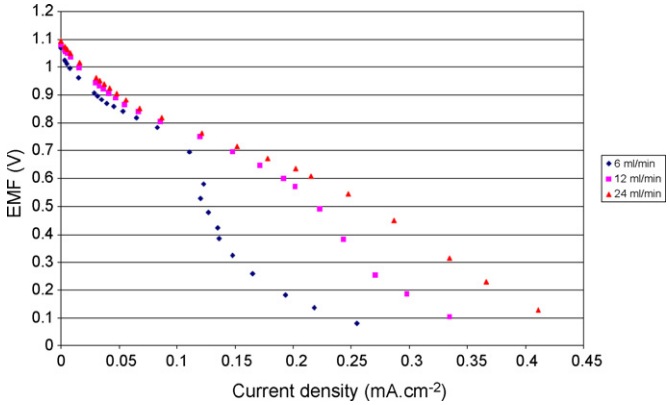

Fig. 10. Influence of the ammonia flow rate on the EMF of a Ag/CaSZ/Ag cell at 873 K.

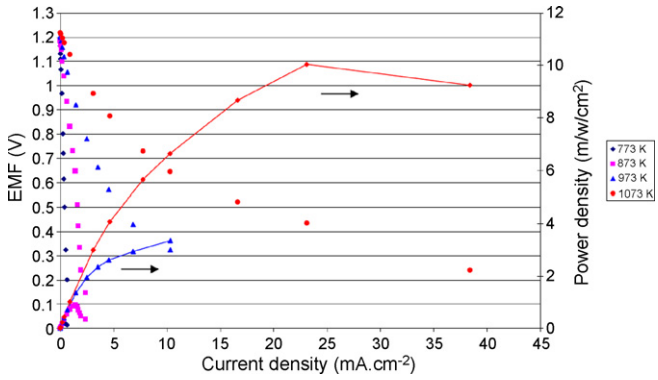

Fig. 11. *I–V* and *I–P* curves of a NiO–YSZ/YSZ/Ag tube.

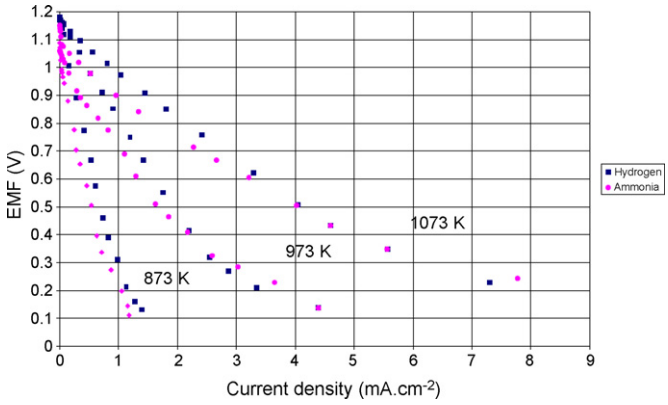

Fig. 12. *I–V* of Ag/YSZ/Ag cell using hydrogen and ammonia as source fuel.

3.1.5. Influence of the temperature

Fig. 11 illustrates the direct influence of the temperature on the performance of the cell. The net improvements of the current densities achieved by the cell are related to higher oxide ion conductivity and a greater conversion of ammonia. The temperature dependency of the ionic conductivity follows Arrhenius' equation [19]:

$$\sigma = \frac{\sigma_0}{T} \exp\left(-\frac{E}{kT}\right),$$

where E is the activation energy, T is the absolute temperature, σ_0 is a material constant and k is the Boltzmann constant. This results in much higher conductivity as the operating temperature of the cell is increased, meaning that the diffusion rate of the oxygen through the electrolyte will be higher and therefore the efficiency of the cell. The other factor responsible for the better performance of the cell is the higher percentage of ammonia decomposed as the temperature increases. It has been shown in an earlier paragraph that the amount of ammonia converted to hydrogen becomes more important, resulting in higher current densities. The limitations in power densities are no longer due to the lack of hydrogen in the cell but to the lack of oxygen transported to the triple phase boundary. The conductivity of the electrolyte material is too low. Indeed, the analysis of the exit gas stream using the mass spectrometer revealed that most of the hydrogen that was produced from the cracking was unconverted, suggesting that diffusion polarization is limiting the performance of the cell, which is not so surprising given the thickness of the electrolyte tube.

3.1.6. Comparison ammonia–hydrogen

The direct performance comparison between hydrogen and ammonia as a fuel at 873, 973 and 1073 K is depicted in Fig. 12. As the temperature increases the performance of the cell running on ammonia approaches the performance of the cell using hydrogen as source fuel. The explanation for this behaviour is given by the fact that ammonia's conversion increases significantly as the temperature rises. The anode atmosphere of the cell using ammonia sees its ammonia partial pressure decrease and its hydrogen partial pressure increase; the two cells have therefore a similar behaviour. In addition to this, mass spectrometer analysis revealed that not all the hydrogen produced from ammonia cracking was consumed in the cell. Diffusion limitation at the cathode is restricting the amount of oxygen available at the triple phase boundary to react with hydrogen.

3.2. Pellet reactor

3.2.1. Influence of the temperature

The same experiments as with the annular system were carried out using the pellet set-up. The influence of the temperature on the behaviour of the cell is presented in Fig. 13.

A similar trend to what was previously observed with the annular cell is obtained with the pellet system. Higher current densities are achieved due to the lower thickness of the pellet, reducing the effect of the poor ionic conductivity of YSZ. The influence of the flow rate and concentration of ammonia were also studied but they did not show any significant effect on the behaviour of the cell. Therefore all experiments were carried out with a flow rate of ammonia of 40 ml min^{-1} which corresponds to a concentration of 50% in the total flow.

3.2.2. Comparison ammonia–hydrogen

Experiments were carried out with a Ni–YSZ/YSZ/Ag system, to determine whether the previously observed trends would be similar in a system with much increased ammonia conversion.

A remarkable result can be observed on Figs. 14 and 15. Pure ammonia gives slightly higher power densities than pure hydrogen when operating at temperatures above 973 K. The difference

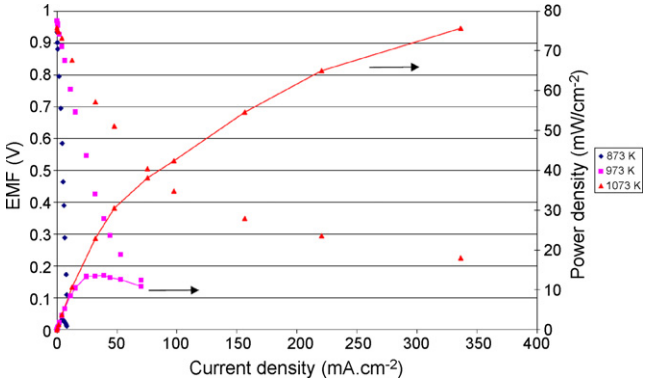

Fig. 13. *I–V* curves of a NiO–YSZ/YSZ/Ag with a 0.4 mm thick pellet.

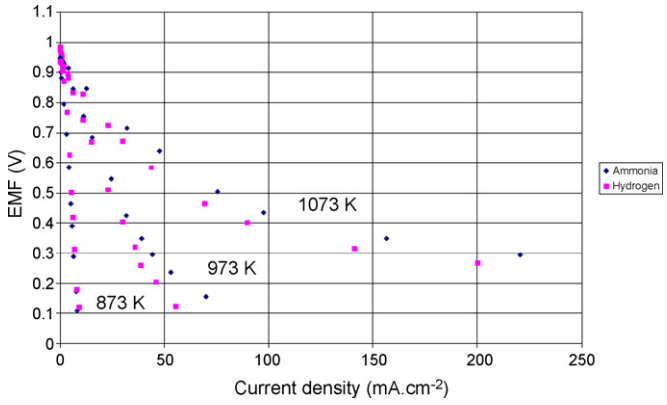

Fig. 14. *I–V* of NiO–YSZ/YSZ/Ag cell using hydrogen and ammonia as source fuel.

between hydrogen and ammonia is approximately 11 mW cm^{-2} for a single cell as shown on Fig. 15, which amounts to some 17% increase. This is entirely due to the choice of anode material, i.e. a nickel cermet which catalyses the decomposition of ammonia and allows for higher conversions. This effect was observed in both annular and pellet system at temperatures above 973 K. Below this temperature, hydrogen gives better performance than ammonia as not enough hydrogen is being produced at the anode. This difference between the two gases can be explained by calculating the equilibrium constant of the reaction in the Nernst equation,

$$E = E^{\circ} - \left(\frac{RT}{nF}\right) \ln(K) \tag{2}$$

The gas compositions on the anode side are very much different when considering ammonia or hydrogen as source fuel.

The gas composition can be calculated using ammonia and hydrogen concentrations (from mass spectrometer). Let us consider a system with a nickel cermet anode: if 1 mol of pure ammonia enters the cell, 92% is converted to hydrogen and nitrogen and 20% of the hydrogen is used, it is possible to calculate the mole fraction for each gas and then evaluate its activity using the following expression:

$$a_i = x_i \phi_i P \tag{3}$$

The calculations of the fugacities are given in Appendix A

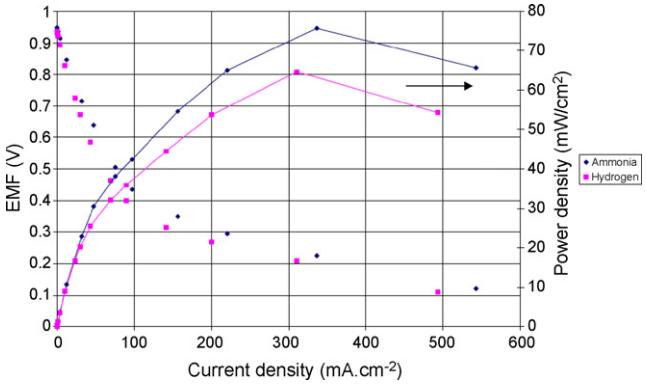

Fig. 15. Ammonia vs. Hydrogen in the pellet cell, NiO–YSZ/YSZ/Ag, at 800 °C.

The mole fraction of ammonia, nitrogen, hydrogen and water are as follows:

$$x_{NH_3} = 0.042, \qquad x_{N_2} = 0.24, \qquad x_{H_2} = 0.575,$$

$$x_{H_2O} = 0.144$$

In the case of pure hydrogen the mole fractions are:

$$x_{H_2} = 0.8, \qquad x_{H_2O} = 0.2$$

The equilibrium constant for pure hydrogen is the following one:

$$K_1 = \frac{a_{H_2O}}{a_{H_2} a_{O_2}^{1/2}} \tag{4}$$

The equilibrium constant for an ammonia system is as follows:

$$K_2 = \frac{a_{N_2}^{1/4} a_{H_2O}}{K a_{NH_3}^{1/2} a_{O_2}^{1/2}}, \tag{5}$$

where K is the equilibrium constant of the decomposition reaction of ammonia into hydrogen and nitrogen at 1073 K.

If K_1 and K_2, from the Nernst equations for a cell using hydrogen or ammonia, are compared, assuming that the oxygen activity coefficient is constant, we obtain $K_1 = 0.2498$ and $K_2 = 0.0085$. The lower value of K_2 implies that the logarithm in the Nernst equation has a higher absolute value, which will contribute to a higher potential E, explaining the experimental observations.

3.3. Comparison with ammonia fuel cells from literature

Ammonia has been used as a direct source fuel in several systems. Metkemeijer [20,21] was the first to report the high potential of ammonia as source fuel in a fuel cell but using an indirect system; a reformer was used to decompose ammonia prior to entering the cell. Wojcik et al. [13] were the first to publish work on a direct ammonia fuel cell using yttria stabilized zirconia as electrolyte material and silver and platinum as electrodes. More recently, Dekker et al. have reported on the use of an anode (NiO–YSZ/YSZ/LSM) supported fuel cell [15].

The systems used have shown different degrees of performance but all confirmed the high potential of ammonia. Fig. 16

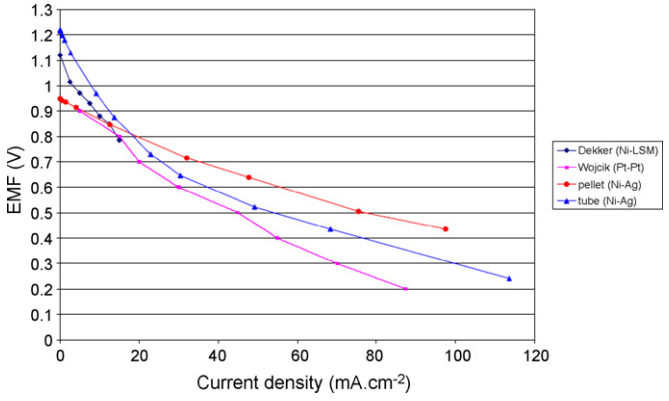

Fig. 16. Normalised *I–V* curves of high performance fuel cell systems using ammonia.

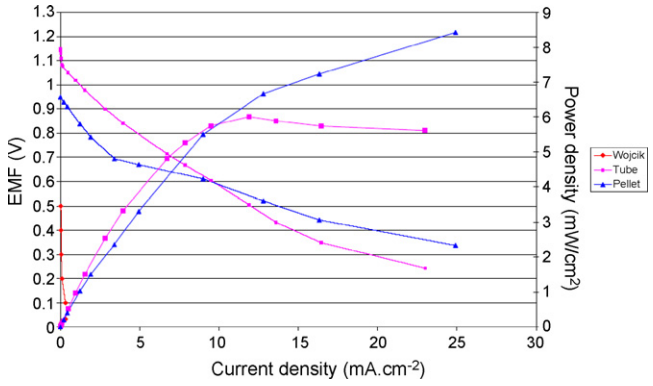

Fig. 17. Normalised *I–V* and *I–P* curves for Ag/YSZ/Ag systems.

presents a comparison of the performance of the different cell configuration normalized to the thickness of the electrolyte material as it is the main source of limitation within the cell at 1073 K. The reference material was 8 mol% yttria stabilized zirconia, which has a resistivity of approximately 20 Ω cm [17] at 1073 K with a thickness of 0.4 mm and the resistivity of 6 mol% yttria stabilized zirconia was taken to be 30 Ω cm at 1073 K. The current densities of the cells with a thinner or thicker electrolyte were multiplied by a proportional factor given by: $L/0.4$, where L is the thickness of the electrolyte in cm when the electrolyte material was 8 mol% YSZ. As per the 6 mol% YSZ tube, the proportional factor was adjusted considering the different conductivity, i.e. multiplied by 1.5, the ratio of the conductivities.

The results obtained with the silver electrodes were too low to be put on the same graph and are shown on Fig. 17. Nickel anodes appear to achieve the best results, which are in agreement with previous studies that demonstrate the high catalytic activity of nickel towards ammonia decomposition [4] and the results found in this study. Furthermore, the pellet design generates the highest current densities for a given potential compared to the annular design: at 0.6 V, the pellet generates 55 mA cm^{-2}, the tube 35 mA cm^{-2} and Wojcik cell's 30 mA cm^{-2}. Dekker et al. did not present any data for voltages below 0.8 V, however the EMF achieved by his cell is lower than those obtained for our annular design.

Fig. 17 shows the results obtained with Ag/YSZ/Ag, which have been normalised using the same method as in the previous graph. It demonstrates again that the best power densities are achieved with the pellet design, but also the poor performance of an Ag/YSZ/Ag system compared to the other systems. At 0.6 V, the cell only achieves 8 mA cm^{-2}. Silver is not an adequate electrode material for direct ammonia fuel cells due to its low ammonia conversion and high cost.

4. Conclusions

The potential use of ammonia in a solid oxide fuel cell has been demonstrated. This was achieved using two very different systems: an annular cell and a pellet. The pellet achieved significantly higher power densities due to a reduced thickness of the electrolyte material. The operating temperature is required to be at least as high as 973 K to obtain a satisfying conversion of ammonia and therefore provide enough hydrogen to the system to achieve maximum power output. The use of noble metals has shown their limitation towards ammonia decomposition and silver and platinum are not suitable as anode materials when using ammonia as direct source fuel. On the other hand, a nickel-based anode is a very efficient material to obtain a high ammonia decomposition. Furthermore, it shows that it is possible to achieve greater power densities with ammonia than using hydrogen as fuel. A difference of 11 mW cm^{-2} was observed at 1073 K between ammonia and hydrogen (in favour of ammonia). Systems such as nickel cermet anode supported fuel cells are good candidates for direct ammonia fuel cells, given the high activity of nickel towards ammonia and the extremely thin electrolyte layers that can be achieved.

Acknowledgements

One of the authors (GF) would like to acknowledge financial support by the Engineering and Physical Science Research Council in the form of studentship.

Appendix A

The fugacities can be calculated using Van der Waals equation of state:

$$P = \frac{RT}{V_i - b} - \frac{a}{V_i^2} \tag{A.1}$$

$$f_i = \phi_i \times P \tag{A.2}$$

$$a = \frac{27}{64}\frac{(RT_c)^2}{P_c}; \tag{A.3}$$

$$b = \frac{RT_c}{8P_c} \tag{A.4}$$

It can be shown using the definition of fugacity that:

$$\ln(f_i) = \ln\left(\frac{RT}{V_i - b}\right) + \frac{b}{V_i - b} - \frac{2a}{RTV_i} \tag{A.5}$$

$$\ln(\phi_i) = \ln\left(\frac{f_i}{P}\right) = -\ln\left[\frac{(V_i - b)P}{RT}\right] + \frac{b}{V_i - b} - \frac{2a}{RTV_i} \tag{A.6}$$

See Tables A.1 and A.2.

Table A.1
Critical temperature and critical pressure [22], calculated a and b parameters for the gases in the cell

Gas	T_c (K)	P_c (Pa)	a (J m^3 mol^{-2})	b (m^3 mol^{-1})
N_2	126.2	3.40×10^6	0.14	3.86×10^{-5}
H_2	33.19	1.31×10^6	0.02	2.63×10^{-5}
NH_3	405.7	1.13×10^7	0.43	3.74×10^{-5}
H_2O	647.1	2.21×10^7	0.55	3.05×10^{-5}

Table A.2
Calculated volume and fugacity for the gases present in the cell

Gas	Vi (m^3)	ϕi
N_2	8.81×10^{-2}	1.000260268
H_2	8.81×10^{-2}	1.000273287
NH_3	8.80×10^{-2}	0.999877441
H_2O	8.80×10^{-2}	0.999650744

References

[1] J.H. Hirschenhoffer, D.B. Stauffer, R.R. Engleman, Fuel Cells: a handbook, in: Business Technology Books, Orinda, California, 1996, pp. 66–69.
[2] N.M. Sammes, R. Boersma, J. Power Sources 86 (2000) 98–110.
[3] K. Kordesch, G. Simader, Fuel Cells and Their Applications, Cambridge, VCH, Weinheim, 1996.
[4] T.V. Choudhary, C. Sivadinarayana, D.W. Goodman, Chem. Eng. J. 93 (2003) 69–80.
[5] FDC, Fertilizer Statistics Report, Muscle Shoals, Alabama, USA, 2001.
[6] G. Shnitkey, Increases in fuel related costs lead to higher production costs, Machinery cost estimates, University of Illinois, USA, 2003.
[7] M.K. Mann, J.S. Ivy, Technology advancements could make solar-derived hydrogen, with its potential for near-site delivery, cost-competitive, Solar Today, May–June 2004.
[8] I.W. Kaye, D.P. Bloomfield, Portable ammonia powered fuel cell, Conference of Power Source, Cherry Hill, pp. 408–409, 1998.
[9] Material safety data sheet for ammonia, Air Liquide, 2002.
[10] C.H. Christensen, T. Johannessen, R.Z. Sorensen, J.K. Norskov, Towards an ammonia mediated hydrogen economy, Catal. Today 111 (2006) 140–144.
[11] V. Hacker, K. Kordesch, Ammonia crackers, Handbook of Fuel CellsFundamentals, in: Technology and Applications, John Wiley and Sons Ltd., Chichester, UK, 2003, pp121–127.
[12] A.S. Chellappa, C.M. Fischer, W.J. Thomson, Appl. Catal. A: Gen. 227 (2002) 231–240.
[13] A. Wojcik, H. Middleton, I. Damopoulos, J.V. Herle, J. Power Sources 118 (2003) 342–348.
[14] N. Maffei, L. Pelletier, J.P. Charland, A. McFarlan, J. Power Sources 140 (2005) 264–267.
[15] N. Dekker, B. Rietveld, Highly efficient conversion of ammonia in electricity by solid oxide fuel cells, in: Proceedings of the 6th European Solid Oxide fuel cell forum, Lucerne, Switzerland, 2004.
[16] T.V. Choudhary, D.W. Goodman, Catal. Today 77 (2002) 65–78.
[17] A.K. Shukla, V. Sharma, N. Arul Dhas, PatilF K.C., Mater. Sci. Eng. B40 (1996) 153–157.
[18] J. Gong, Y. Li, Z. Tang, Z. Zhang, Mater. Lett. 46 (2000) 115–119.
[19] J.A. Kilner, B.C.H. Steele, Nonstoichiometric Oxides, Academic Press, 1981, pp 233.
[20] R. Metkemeijer, P. Achard, Int. J. Hydrogen Energy 19 (1994) 535–542.
[21] R. Metkemeijer, P. Achard, J. Power Sources 49 (1994) 271–282.
[22] CRC Handbook of Chemistry and Physics, 60th ed.